FACULTY OF PHYSICS
UNIVERSITY OF WARSAW

Stability of domain walls in BSM models with asymmetric potentials

Zygmunt Lalak
ITP Warsaw

with **M. Lewicki, P. Olszewski, T. Krajewski,**
O. Czerwińska, Ł. Nakonieczny, J. Kwapisz

arXiv:1402.3826 (JHEP), arXiv: 2103.03225, arXiv:1605.06713 (PRD),
arXiv:1411.6435 (PRD), arXiv:1606.07808 (JHEP), arXiv:1508.03297 (JHEP)
arXiv:1608.05719 (JCAP), arXiv:1711.08473 (JHEP)

Corfu Summer Institute, September 2021

Outline:

- SM and BSM effective potentials with non-equivalent vacua
- Domain walls
- Domain walls at finite temperature
- Domain walls and gravitational waves
- Summary

Models of interest

- Radiatively generated minima (eg SM at large field strength)

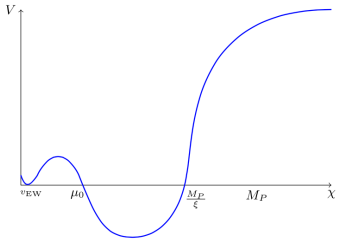

- Run-away potentials (moduli of stringy models), Quantum Scale Symmetric SM

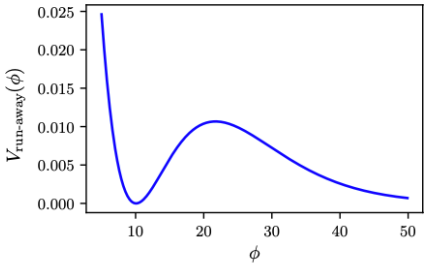

- Models of strong first-order phase transitions - colliding bubbles (thermal effects play a role)

Models of interest

- Monodromy axion models, relaxion

$$V_{\text{monodromy}}(\phi) = m^2\phi^2 + \Lambda^4\left[1 - \cos\left(\frac{\phi}{f}\right)\right]$$

$$V_{\text{relaxion}}(\phi) = g\phi + \Lambda^4\left[1 - \cos\left(\frac{\phi}{f}\right)\right]$$

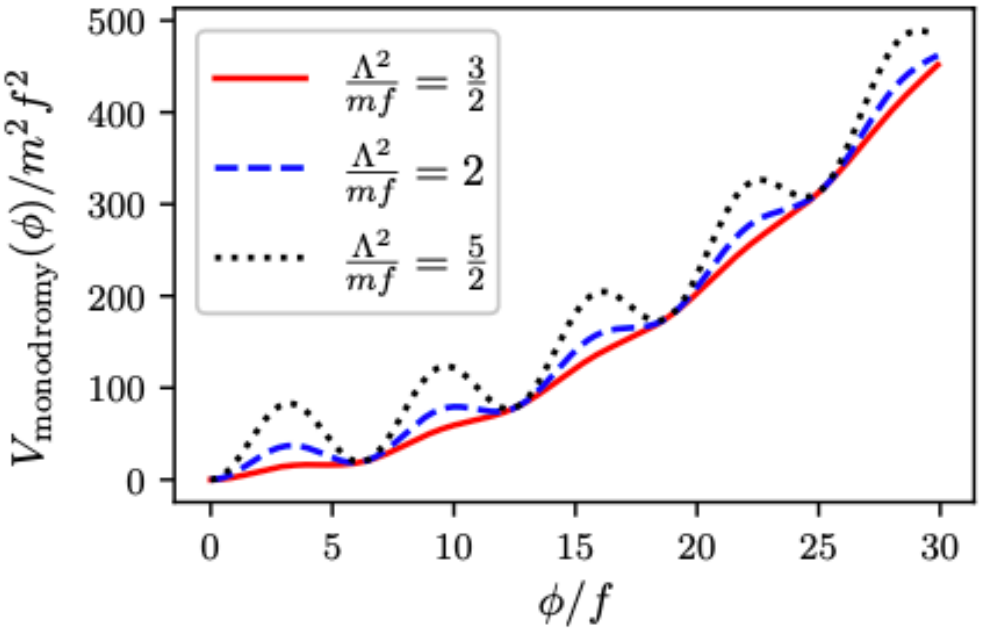

SM Effective potential

Standard Model Effective potential

$$V_{SM}(\mu) = -\frac{m^2}{2}\phi^2 + \frac{\lambda}{4}\phi^4 + \sum_i \frac{n_i}{64\pi^2} M_i^4 \left[\ln\left(\frac{M_i^2}{\mu^2}\right) - C_i \right]$$

For large field values $m^2 << \phi^2$ and $\mu = \phi$ the potential is very well approximated by

$$V_{SM}(\phi) \approx \phi^4 \left\{ \frac{\lambda}{4} + \frac{1}{64\pi^2} \left[6\left(\frac{g_2^2}{4}\right)^2 \left(\ln\left(\frac{g_2^2}{4}\right) - \frac{5}{6}\right) + 3\left(\frac{g_1^2+g_2^2}{4}\right)^2 \left(\ln\left(\frac{g_1^2+g_2^2}{4}\right) - \frac{5}{6}\right) \right.\right.$$
$$\left.\left. -12\left(\frac{y_t^2}{2}\right)^2 \left(\ln\left(\frac{y_t^2}{2}\right) - \frac{3}{2}\right) + \left(\frac{3\lambda}{2}\right)^2 \left(\ln\left(\frac{3\lambda}{2}\right) - \frac{3}{2}\right) + 3\left(\frac{\lambda}{2}\right)^2 \left(\ln\left(\frac{\lambda}{2}\right) - \frac{3}{2}\right) \right] \right\}$$

$$V_{SM}(\phi) \approx \frac{\lambda_{eff}(\phi)}{4}\phi^4$$

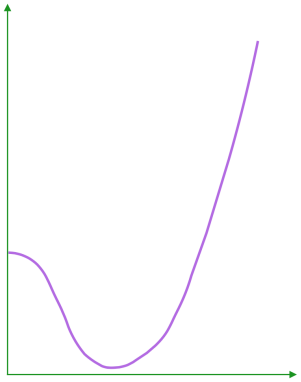

classically ← → quantum corrected ...

SM Metastability

$$\lambda_{eff} < 0 \Longrightarrow \text{Metastability}$$

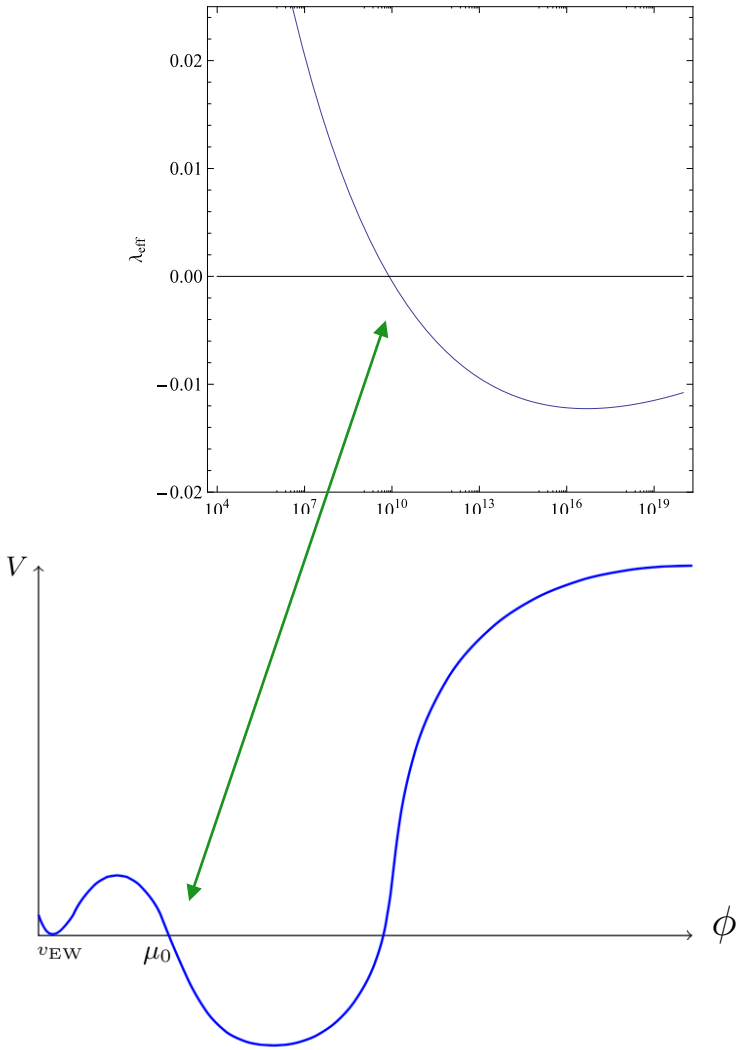

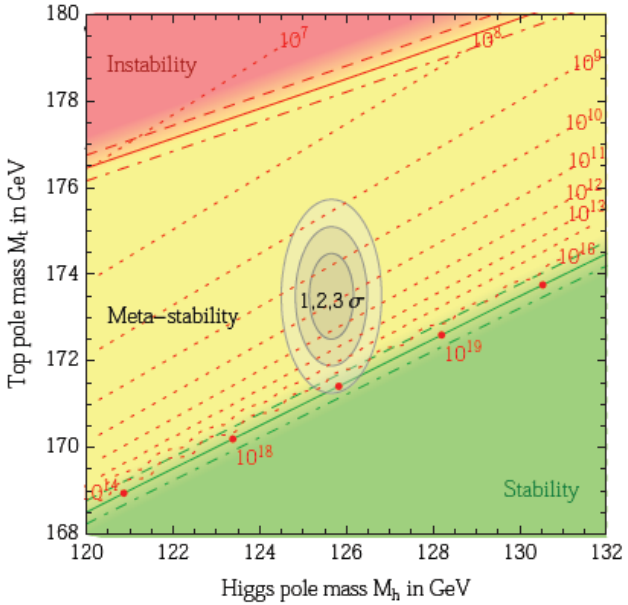

D. Buttazzo, et al. [arXiv:1307.3536].
G. Degrassi, et al. [arXiv:1205.6497].

See lectures by G. Degrassi Corfu 2014

Magnitude of the suppression scale

Approximate lifetime:

$$\frac{\tau}{T_U} = \frac{1}{\mu^4(\lambda_{min})\, T_U^4} e^{\frac{8\pi^2}{3|\lambda_{min}|}}.$$

Positive λ_6 and $\lambda_8 \rightarrow$ stabilizing the potential

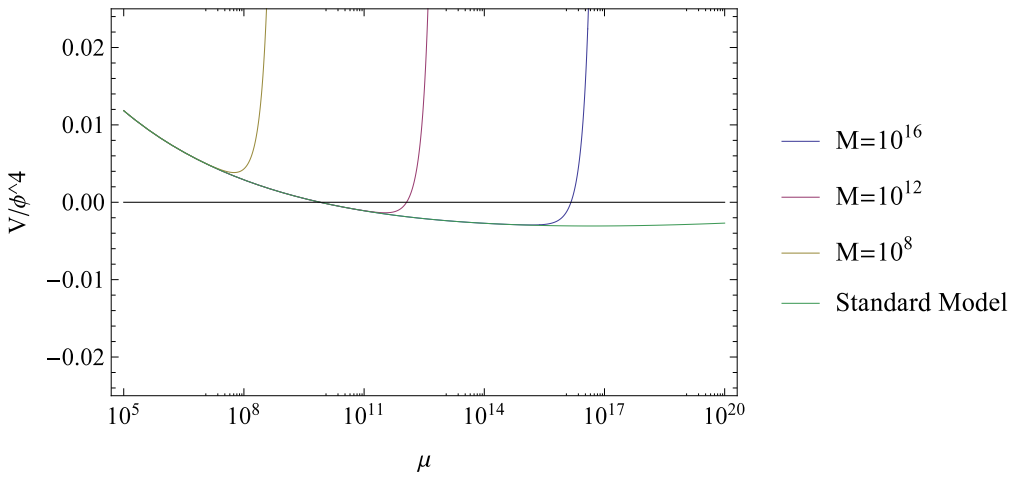

Figure: Scale dependence of $\frac{\lambda_{eff}}{4} = \frac{V}{\phi^4}$ with $\lambda_6 = \lambda_8 = 1$ for different values of suppression scale M. The lifetimes corresponding to suppression scales $M = 10^8, 10^{12}, 10^{16}$ are, respectively, $\log_{10}(\frac{\tau}{T_U}) = \infty, 1302, 581$ while for the Standard Model $\log_{10}(\frac{\tau}{T_U}) = 540$.

Magnitude of the suppression scale

Positive λ_8 and negative $\lambda_6 \rightarrow$ New Minimum

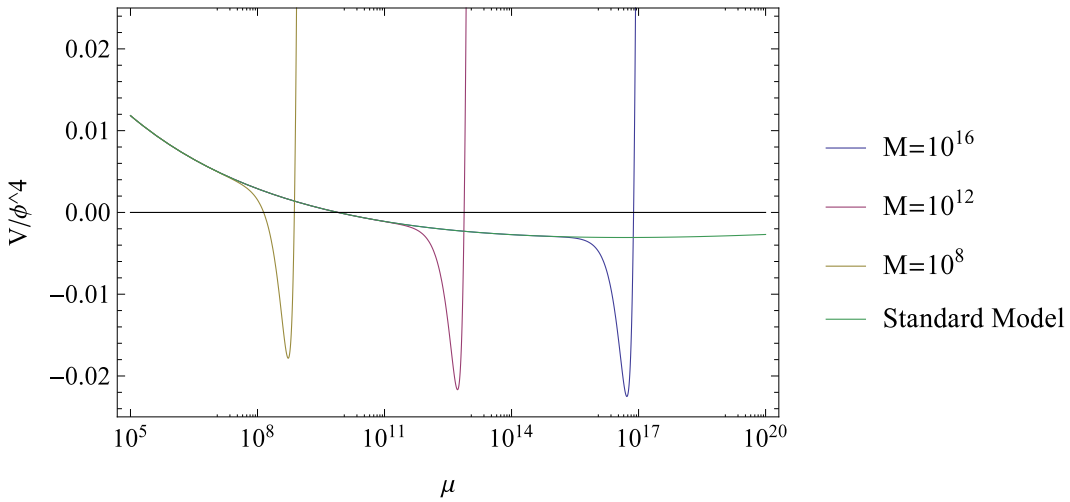

Figure: Scale dependence of $\frac{\lambda_{eff}}{4} = \frac{V}{\phi^4}$ with $\lambda_6 = -1$ and $\lambda_8 = 1$ for different values of suppression scale M. The lifetimes corresponding to suppression scales $M = 10^8, 10^{12}, 10^{16}$, are, respectively, $\log_{10}(\frac{\tau}{T_U}) = -45, -90, -110$ while for the Standard Model $\log_{10}(\frac{\tau}{T_U}) = 540$.

SM + dilaton

Quantum scale symmetric effective lagrangian

See talks by G.G. Ross and D. Ghilencea

No scale anomaly in

„*dynamical*" *regulator*

$$\mathcal{L}^{(0)}(\phi,\sigma) = \frac{1}{2}(\partial\phi)^2 + \frac{1}{2}(\partial\sigma)^2 - \mu^{2\varepsilon}(\sigma)\left[\underbrace{V(\phi,\sigma)}_{\text{renormalizable, classicaly scale-invariant}} + \sum_{n=0}\lambda_n\frac{\phi^{4+2n}}{\sigma^{2n}}\right]$$

$\mathbb{Z}^2 \times \mathbb{Z}^2$

$\phi \to -\phi$

$\sigma \to -\sigma$

go to *broken phase*

$$\mathcal{L}^{(0)}(\phi_0+\phi', \sigma_0+\phi')$$

compute loop corrections (in momentum expansion) & RGE functions *β, γ*

$$\mathcal{L}_{\text{eff}}(\phi,\sigma) = -V_{\text{eff}}(\phi,\sigma) + \ldots$$

- Homogenous function (no mass-parameters, only vev's)
- $\mathbb{Z}^2 \times \mathbb{Z}^2$ sym.
- Satisfies Callan-Symanzik eq.

Quantum scale symmetric effective lagrangian

RG-improvement:

$$\mu = e^t \mu_0 \,, \qquad \lambda(t)\,\phi^4 + \frac{\lambda^2(t)\phi^4}{64\pi^2}\,\log\left(\frac{\phi}{e^t\sigma}\right)^2 + \dots$$

Choose $t = t(\phi,\sigma) \sim \log\frac{\phi}{\sigma}$ to avoid large logs.

Spontanous scale-symmetry breaking:

$$\begin{pmatrix}\phi\\ \sigma\end{pmatrix} = M\begin{pmatrix}\sin\theta\\ \cos\theta\end{pmatrix}\,, \quad V_{\rm eff} = M^4\,W(\theta)\,,$$

→ flat direction in $V_{\rm eff}$ $\Rightarrow$

$$\exists_{\theta=\theta_0}\, W(\theta_0) = W'(\theta_0) = 0$$

renormalization condition, similar to choosing C.C.

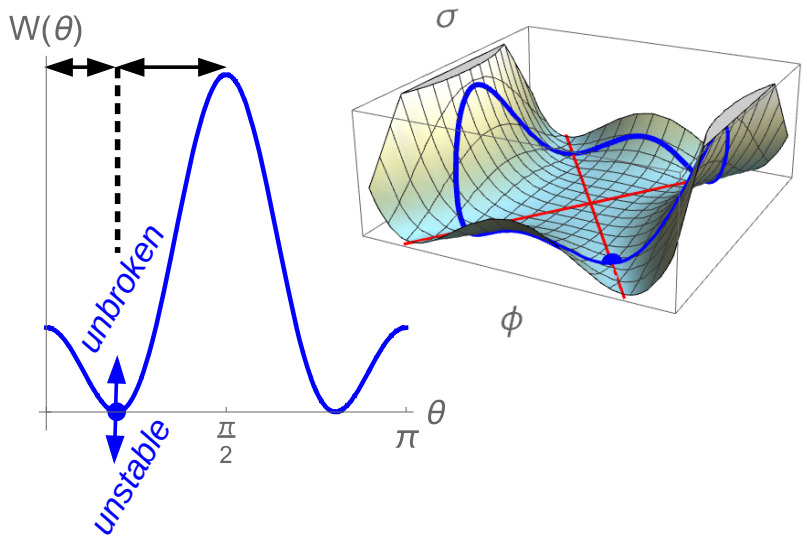

- **Hierarchy** of scales via **aligning** the flat direction $\perp\phi$ → $\theta_0 \approx \frac{\phi_0}{\sigma_0} \ll 1$
- New perspective on **naturalness**: is this alignement stable wrt. embedding in a UV completion?

Quantum scale symmetric SM + σ

$$H = \begin{pmatrix} 0 \\ \frac{\phi}{\sqrt{2}} \end{pmatrix}$$

(electroweak vacuum → electroweak flat direction)

$$\mathcal{L}_{SM}\Big|_{\substack{m^2=0 \\ \mu=\mu(\sigma)}} + \frac{1}{2}(\partial\sigma)^2 - \lambda_m |H|^2\sigma^2 - \frac{\lambda_\sigma}{4}\sigma^4 + \sum_{n=0}\lambda_n \frac{|H|^{4+2n}}{\sigma^{2n}}$$

$$V_{\rm eff}^{\rm SM}(\phi,\sigma) \approx \frac{1}{4}\lambda_{\rm eff}\left(\log\frac{\phi}{\sigma}\right)\phi^4 = M^4 \underbrace{\lambda_{\rm eff}(\log\tan\theta)\frac{\tan^4\theta}{(1+\tan^2\theta)^2}}_{W(\theta)}$$

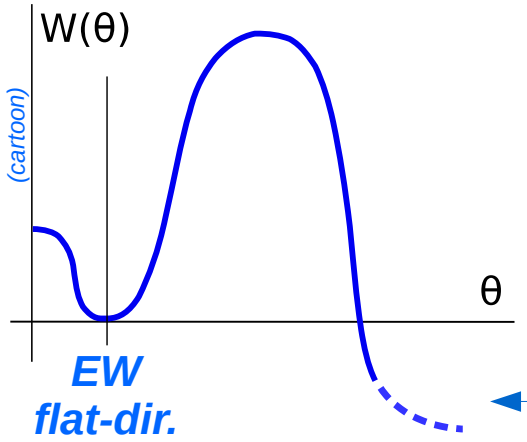

$V_{\rm eff}$ is:

- ***unstable***
- ***unbounded below***

Tunneling via **2-dim instanton** (Coleman's bounce), in the presence of nonrerm. terms.

(Even stronger) motivation to stabilise the ***$V_{\rm eff}$*** completely: $\lambda_{\rm eff} \overset{!}{>} 0$

Summary

SM + dilaton

1) You may use **a field as the scale *μ***
in Dim-Reg to preserve scale symmetry at the quantum level.

2) The price to pay: infinitely many nonpolynomial ϕ/σ operators
and corresponding couplings: **nonrenormalizability**.

3) Minimal subtraction scheme involves **evanescent interactions**.

4) Presence of a **flat direction** $\leftarrow$ tuning.

5) **Naturalness: aligning** the flat direction perpendicular to Higgs

6) **Instability = unboundedness below**

Gravity Corrections in Curved Space

Coleman-De Luccia bounces

$$\mathcal{L} = \frac{1}{2}(\partial\phi)^2 - V, \quad V = -a^2(3b-1)\phi^2 + a(b-1)\phi^3 + \frac{1}{4}\phi^4 + C$$

two minima at $\phi = 0$ and $\phi = 2a$

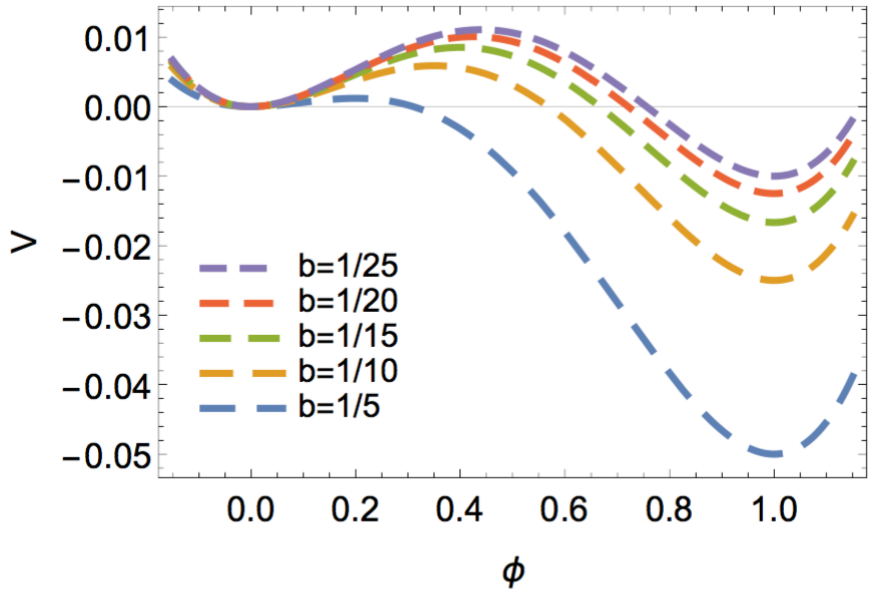

$C = 0$

Figure 1. Our toy model potential for different values of b parameter. In this example vacuum energy vanishes $c = 0$. Different choices of vacuum energy, we will discuss, simply mean adding a constant to the potential.

Transition probability

$$\Gamma = Ae^{-S}$$

$$S_{\text{CDL}} = S[\phi_{\text{CDL}}] - S[\phi_{\text{fv}}]$$

$$S[\phi_{\text{fv}}] = -\frac{24\pi^2}{V_{\text{min}}}, \quad \text{(for dS)}$$
$$S[\phi_{\text{fv}}] = 0, \quad \text{(for Minkowski)}$$

$$ds^2 = d\tau^2 + r(\tau)^2(d\Omega)^2$$

$$S_E = 2\pi^2 \int d\tau \rho^3 \left(\frac{1}{2}\dot{\phi}^2 + V + \frac{1}{2}R \right)$$

$$R = 6\left(\frac{\ddot{\rho}}{\rho} + \left(\frac{\dot{\rho}}{\rho} \right)^2 - \frac{1}{\rho^2} \right) \text{ and } \dot{\phi} = \frac{d\phi}{d\tau}$$

Equations of motion

$$\ddot{\phi} + 3\frac{\dot{\rho}}{\rho}\dot{\phi} = \frac{\partial V}{\partial \phi}$$

$$\dot{\rho} = \sqrt{1 + \frac{\rho^2}{3}\left(\frac{1}{2}\dot{\phi}^2 - V\right)}$$

Boundary conditions

$$\begin{aligned}
\dot{\phi}(0) &= \dot{\phi}(\tau_{\text{end}}) = 0 \\
\rho(0) &= 0 \\
\rho(\tau_{\text{end}}) &= 0, \quad \text{(for dS)} \\
\rho(\tau_{\text{end}}) &= \rho_{\text{end}} \neq 0, \quad \text{(for Minkowski)}
\end{aligned}$$

Hawking-Moss solution

Simpler HM solution S.W. Hawking, I.G. Moss, Phys.Lett. B 110 (1982) describes the probability for a whole spacetime volume to transition simultaneously to the top of the barrier (max) and continue by a classical roll-down:

$$S_{HM} = S_{\max} - S_{fv} =$$
$$= -\frac{24\pi^2(1-\kappa\xi\phi_{\max}^2)^2}{\kappa^2 V_{\max}} + \frac{24\pi^2(1-\kappa\xi\phi_{fv}^2)^2}{\kappa^2 V_{fv}}$$

including the modification coming from ξ

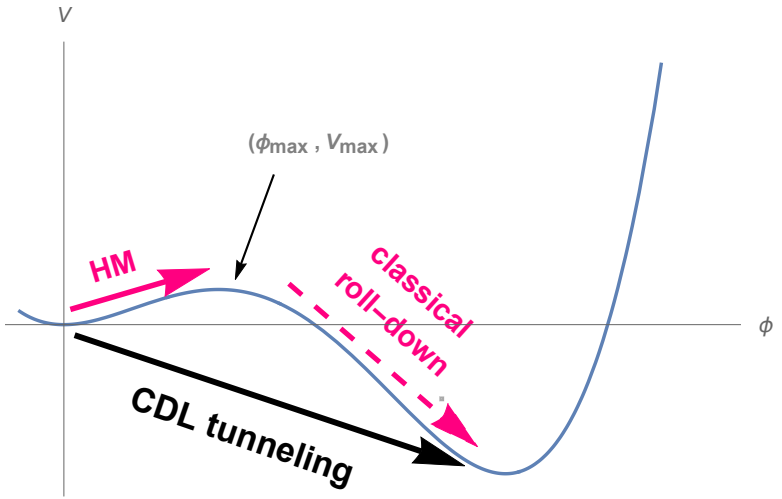

Hawking-Moss vs CDL

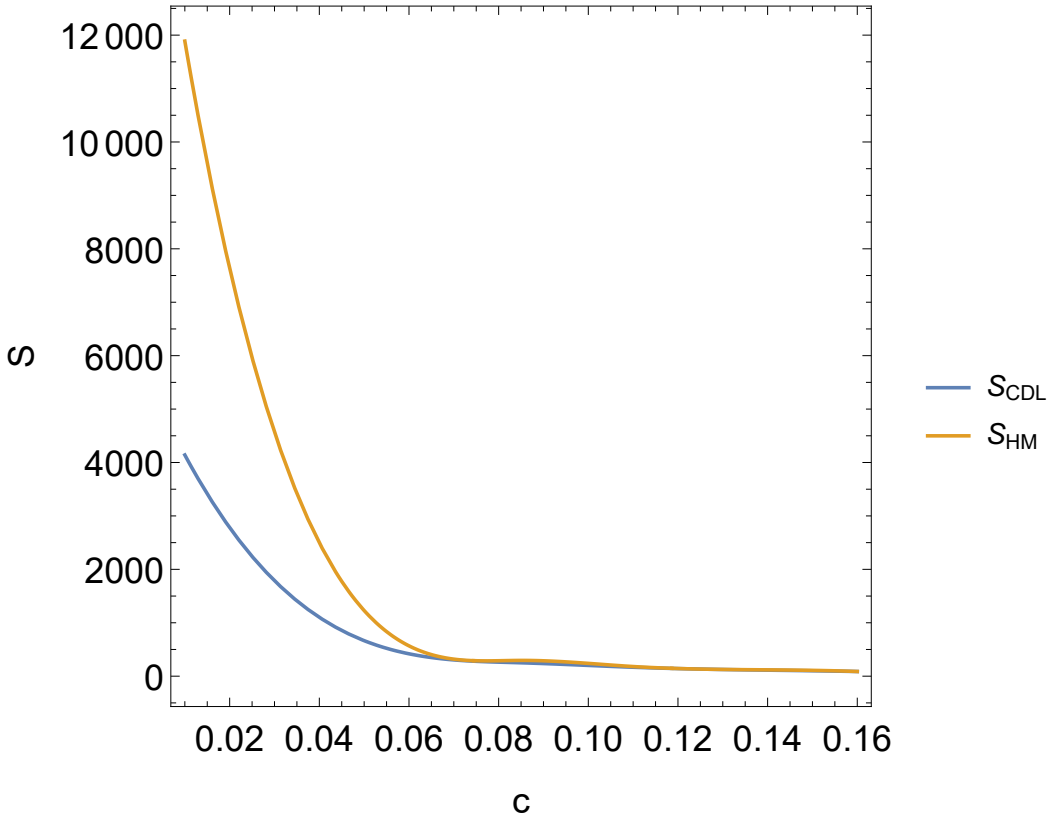

Conclusions CDL

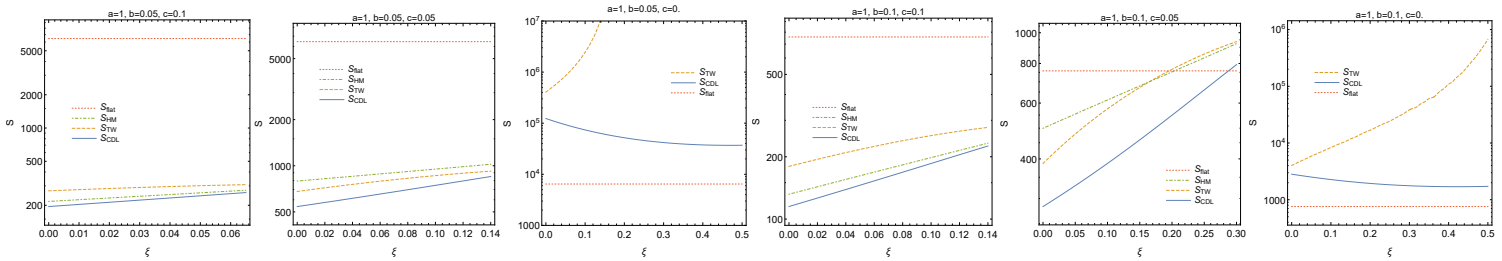

The influence of non-minimal coupling to gravity is very different in cases of Minkowski and dS vacua:

- dS - the decay probability quickly decreases as the coupling grows, vacuum can be made absolutely stable
- Minkowski - effect is much weaker, the decay rate increases for small values, TW approximation works worse significantly overestimating the increase in action due to ξ

Even though TW approximation may not give a precise result in a specific model, the order of magnitude is right (especially in dS case where gravitational correction decreases the stability).

Domain walls

Network of walls prefers the true vacuum!

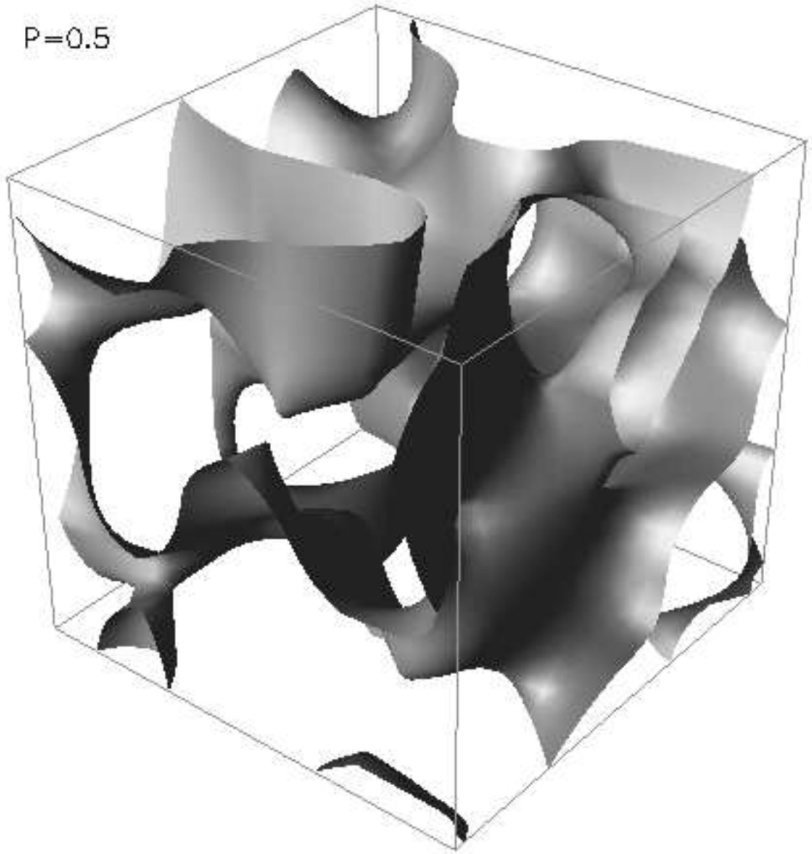

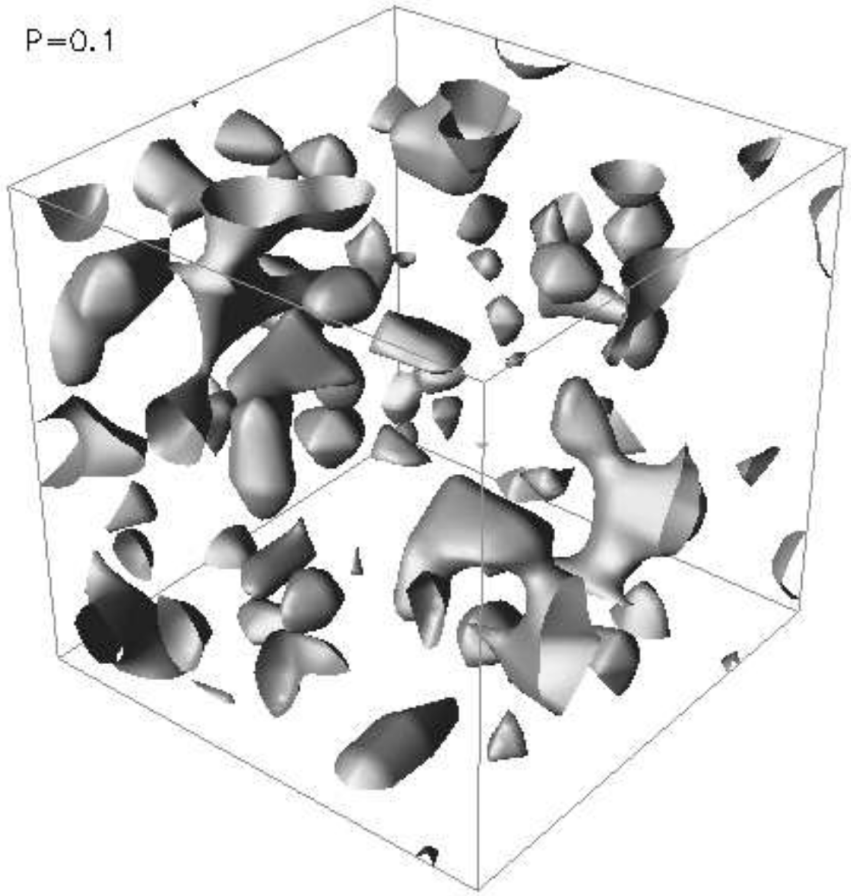

About our simulation

- We modeled the Higgs field with a positive, real scalar ϕ.
- The evolution of ϕ is given by EOM:

$$\frac{\partial^2 \phi}{\partial \eta^2} + \frac{\alpha}{\eta}\left(\frac{d \ln a}{d \ln \eta}\right)\frac{\partial \phi}{\partial \eta} - \Delta\phi = -a^\beta \frac{\partial V}{\partial \phi},$$

  with a potential $V(\phi)$ equal to the RG improved potential of the SM Higgs $V_{\mathrm{SM}}(|h|)$.
- The PRS algorithm[2] (with $\alpha = 3$, $\beta = 0$) was used.
- We used the optimization of a time step[3].
- Our simulations were run on a lattice of the size 512^3.

[2] William H. Press, Barbara S. Ryden, and David N. Spergel. "Dynamical Evolution of Domain Walls in an Expanding Universe". In: *Astrophys. J.* 347 (1989), pp. 590–604. DOI: 10.1086/168151.

[3] Z. Lalak, S. Lola, and P. Magnowski. "Dynamics of domain walls for split and runaway potentials". In: *Phys. Rev.* D78 (2008), p. 085020. DOI: 10.1103/PhysRevD.78.085020. arXiv: 0710.1233 [hep-ph].

Initial conditions

Following the general considerations[4] we assumed that the initial distribution of field strength is given by probability distribution:

$$P(h) = \frac{1}{\sqrt{2\pi}\sigma_I} e^{-\frac{(h-\theta)^2}{2\sigma_I^2}} \quad \sigma_I \sim \frac{\sqrt{N} H_I}{2\pi}$$

We considered various combinations of values of σ and θ in order to cover the set of initial conditions which can be predicted by models of the early Universe.

Our simulations were initialized at different conformal times η_{start} ranging from 10^{-14} GeV^{-1} to 10^{-10} GeV^{-1}.

[4] Z. Lalak et al. "Large scale structure from biased nonequilibrium phase transitions: Percolation theory picture". In: *Nucl. Phys.* B434 (1995), pp. 675–696. DOI: 10.1016/0550-3213(94)00557-U. arXiv: hep-ph/9404218 [hep-ph].

Dependence on the initialization time

For nearly equal contributions of both vacua at the initialization, late domain walls decay longer leading to domination of the EW vacuum even if the fraction of lattice sites occupied by this vacuum decreases initially.

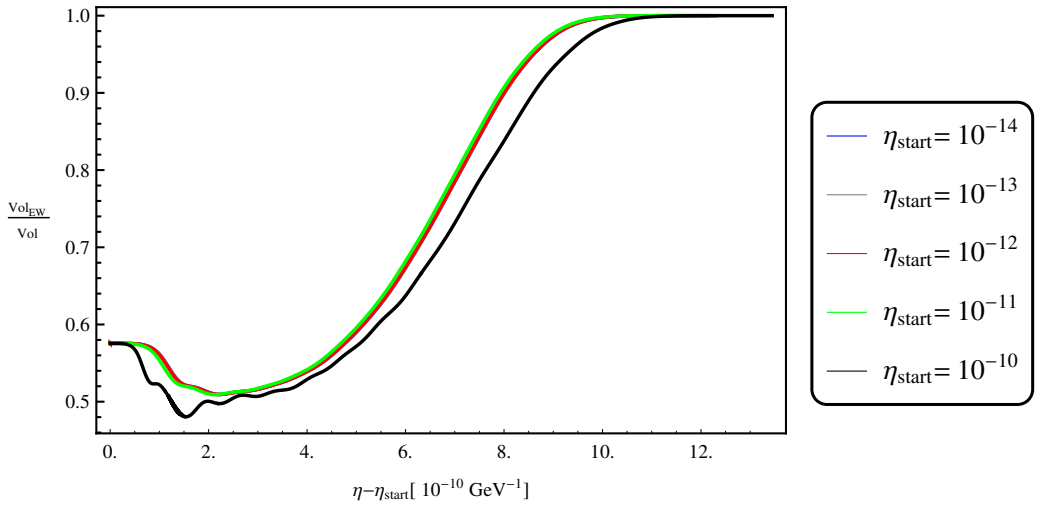

Figure: The fraction $\frac{Vol_{EW}}{Vol}$ as a function of conformal time η for different initialization times η_{start}.

Dependence on the initialization time

The decay of domain walls ending in the state without the EW vacuum is possible even for the initial configuration with a slight dominance of the EW vacuum.

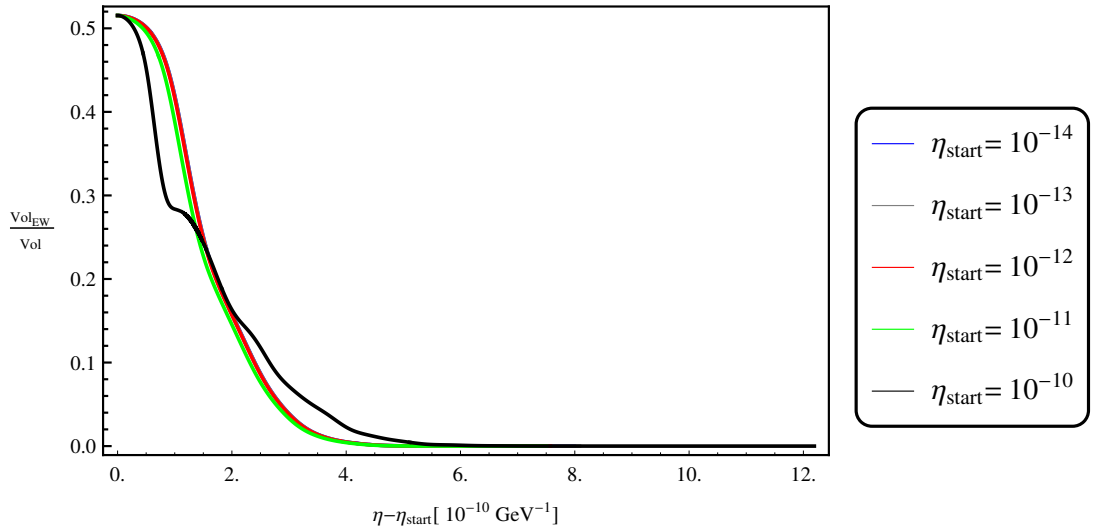

Figure: The fraction $\frac{Vol_{EW}}{Vol}$ as a function of conformal time η for different initialization times η_{start}.

Higgs domain walls after reheating

Higgs domain walls after reheating

- After reheating the early Universe was very hot and dense and it was better described that time by the thermal state with temperature T, than by the vacuum state.
- The dynamics of Higgs domain walls in the background of this thermal state could be different than in the vacuum state.
- The evolution of the domain walls in the cooling down Universe can be determined reliably only in lattice simulations.

Thermal effective potential

$$V_{\text{eff}}(h,T) = \frac{1}{2}m^2h^2 + \frac{1}{4}\lambda h^4 + \sum_{i=\varphi,\chi,W,Z,t} \frac{1}{2}n_i T \sum_{n=-\infty}^{\infty} \int \frac{d^3\vec{k}}{(2\pi)^3} \log\left[\vec{k}^2 + {\omega_n}^2 + {m_i}^2(\phi)\right]$$

$$\begin{aligned}
{m_h}^2(\phi) &= m^2 + 3\lambda h^2, \\
{m_{\chi_i}}^2(\phi) &= m^2 + \lambda h^2, \\
{m_W}^2(\phi) &= \frac{g^2}{4} hi^2, \\
{m_Z}^2(\phi) &= \frac{g^2 + g'^2}{4} h^2, \\
{m_t}^2(\phi) &= \frac{{y_t}^2}{2} h^2,
\end{aligned}$$

$$\begin{aligned}
V_{\text{SM}}(h,T) = \frac{1}{2}m^2h^2 + \frac{1}{4}\lambda h^4 &+ \sum_{i=\varphi,\chi,W,Z,t} n_i \frac{{m_i}^4(h)}{64\pi^2}\left[\log\frac{{m_i}^2(h)}{\mu^2} - C_i\right] \\
&+ \sum_{i=\varphi,\chi,W,Z} \frac{n_i T^4}{2\pi^2} J_b\left(\frac{{m_i}^2(h)}{T^2}\right) + \frac{n_t T^4}{2\pi^2} J_f\left(\frac{{m_t}^2(h)}{T^2}\right) \\
&+ \sum_{i=\varphi,\chi,W,Z,\gamma} \frac{\bar{n}_i T}{12\pi}\left[{m_i}^3(h) - \left({m_i}^2(h) + \Pi_i(T)\right)^{\frac{3}{2}}\right],
\end{aligned}$$

Position of the local maximum

Figure : The position h_{max} of the local maximum separating two minima of the RG improved effective potential as a function of the temperature of thermal bath T.

Width of Higgs domain walls

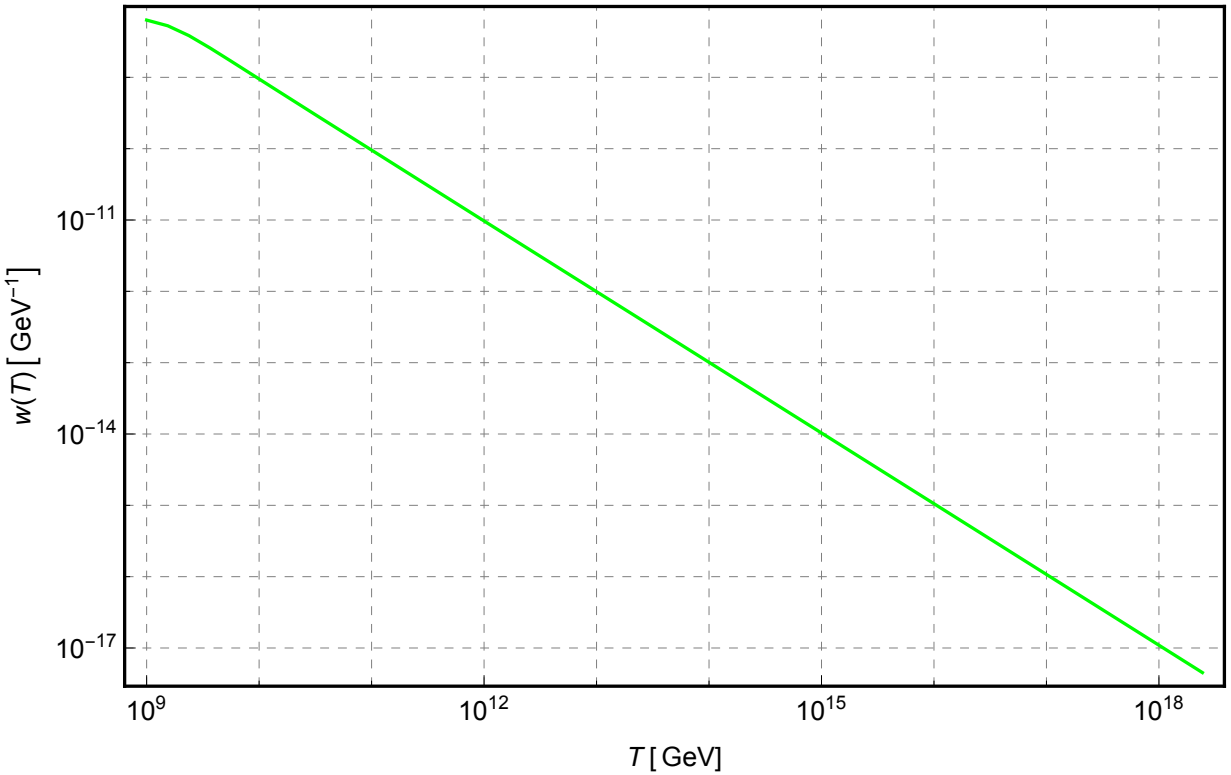

Figure : The width of domain walls w as a function of the temperature T.

Evolution in the thermal background

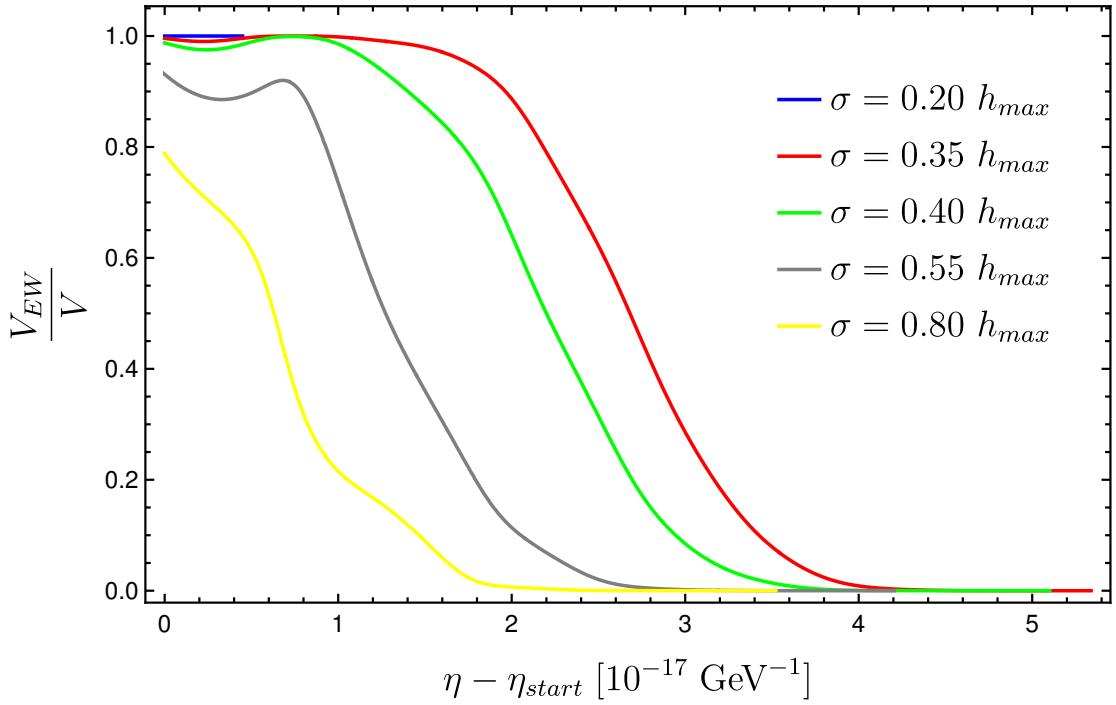

Figure : The fraction $\frac{V_{EW}}{V}$ as a function of conformal time η for values of standard deviation σ of initialization distribution.

Summary - thermal bath

- SM thermal corrections to the effective potential enlarge the basin of attraction of the EWSB vacuum
- Higgs domain walls in the thermal bath are highly unstable

Gravitational waves from domain walls

Gravitational waves from domain walls

Energy density generated by one mode $\varrho_{gw}(\eta, k)$ can be expressed as:

$$\varrho_{gw}(\eta,k) = \frac{1}{16\pi^3 {M_{Pl}}^2 a(\eta)^4 V} \sum_{i,j} \left[\left| \int_{\eta_i}^{\eta_f} d\eta' \cos\left(|k|\left(\eta-\eta'\right)\right) a(\eta') \widehat{T^{TT}}_{ij}(\eta', k) \right|^2 \right.$$
$$\left. + \left| \int_{\eta_i}^{\eta_f} d\eta' \sin\left(|k|\left(\eta-\eta'\right)\right) a(\eta') \widehat{T^{TT}}_{ij}(\eta', k) \right|^2 \right],$$

after redshift

$$\frac{d\rho_{gw}}{d\log|k|}(\eta_0, k) = (1+z_{EQ})^{-4} \frac{a(\eta_{dec})^4}{a(\eta_{EQ})^4} \frac{d\rho_{gw}}{d\log|k|}(\eta_{dec}, k),$$

$$f_0 = \frac{a(\eta_{dec})}{a(\eta_0)} \frac{k}{2\pi} = 5.07 \times 10^6 \left(\frac{10^{19}\,\frac{\mathrm{eV}}{\hbar}}{H_{dec}} \right)^{\frac{1}{2}} \left(\frac{k}{10^{10}\,\frac{\mathrm{GeV}}{\hbar c}} \right) \mathrm{Hz}.$$

Expectations:

N. Kitajima and F. Takahashi, *Gravitational waves from Higgs domain walls*, *Phys. Lett.* **B745** (2015) 112–117, [1502.03725].

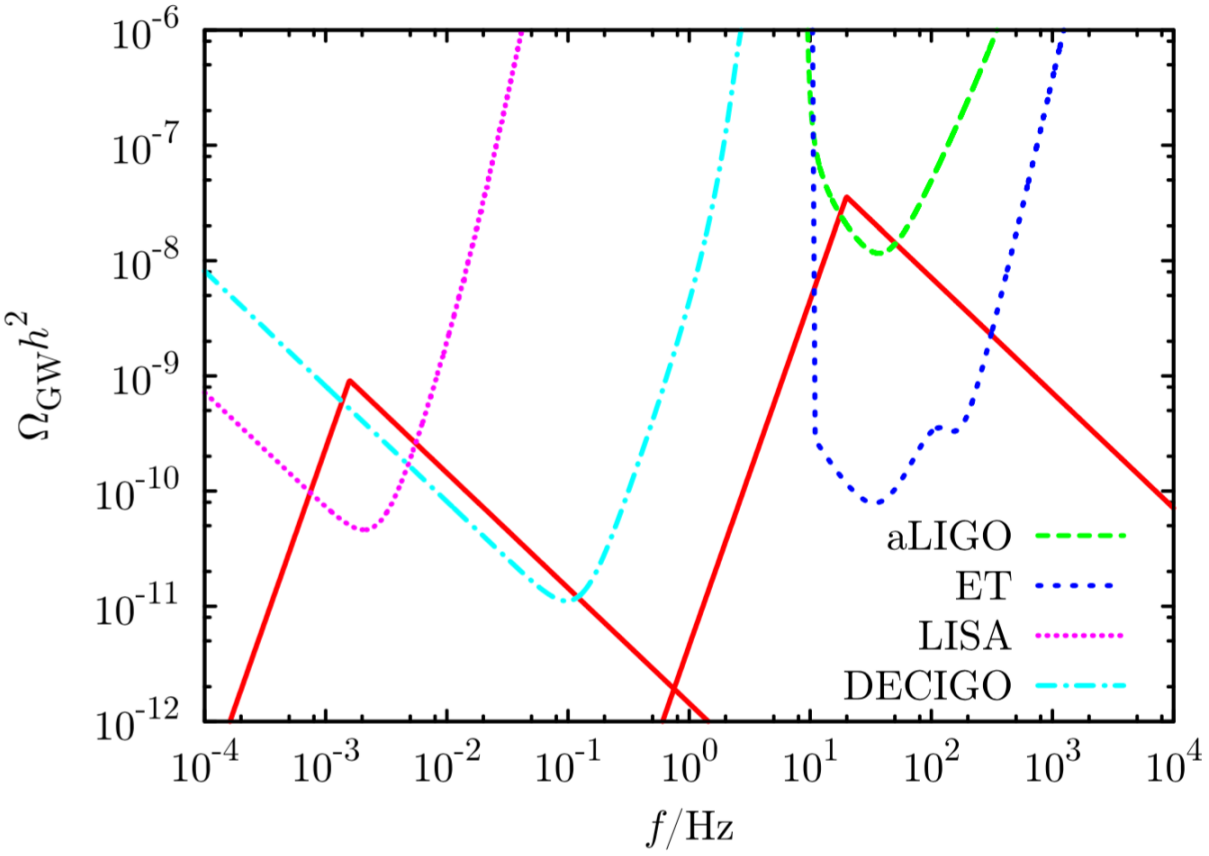

Fig. 3. The typical spectrum of the gravitational waves is shown by the solid (red) lines. We have taken $\varphi_f = 2 \times 10^9$ GeV and $(V_f/V_{\rm max})^{1/4} = 5 \times 10^{-5}$ for the left line and $\varphi_f = 2 \times 10^{12}$ GeV and $(V_f/V_{\rm max})^{1/4} = 10^{-3}$ for the right line.

Numerical simulations:

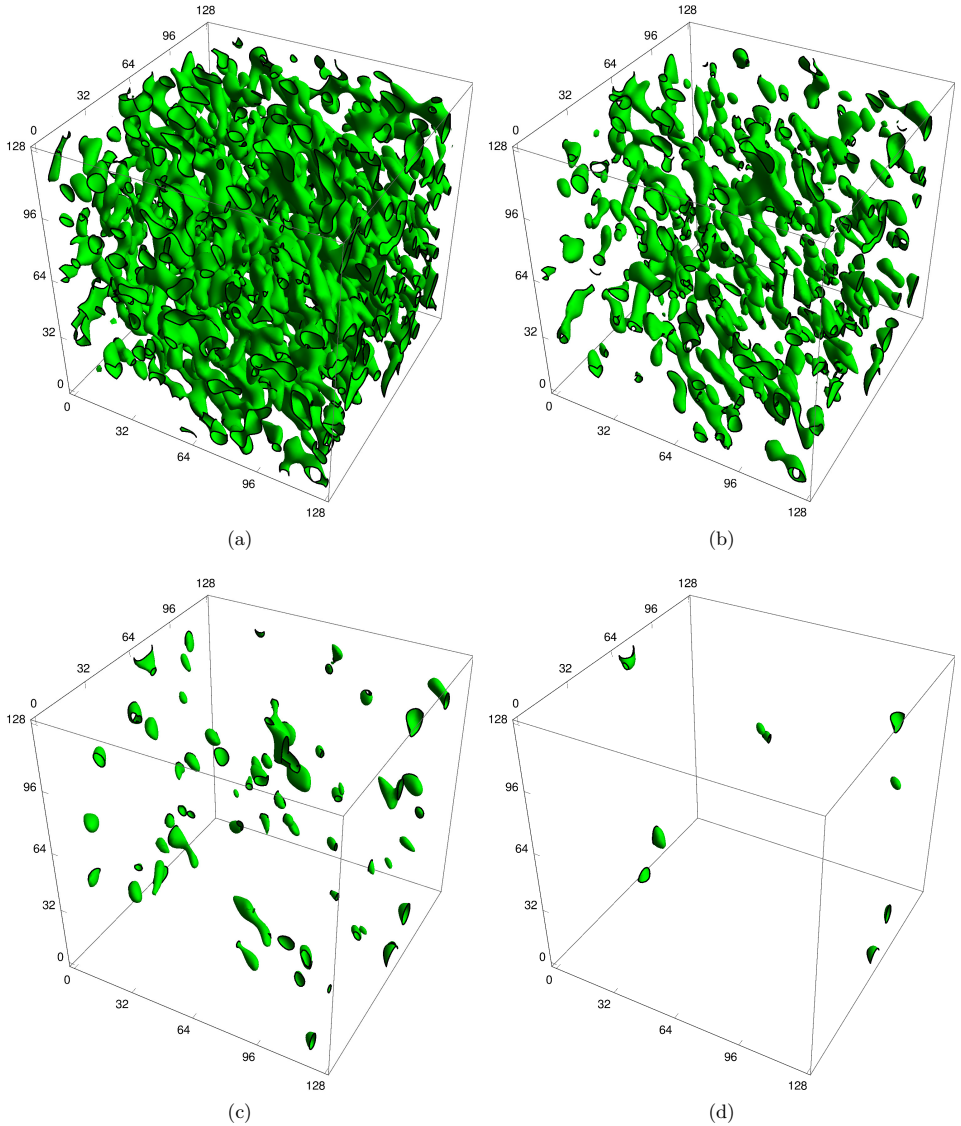

Figure 11: **Visualization of the isosurface of the field strength ϕ corresponding the value v_{max} at four different conformal times: $\eta = 10^{-9}$ GeV^{-1} (a) and $\eta = 1.2 \times 10^{-9}$ GeV^{-1} (b), $\eta = 1.3 \times 10^{-9}$ GeV^{-1} (c), $\eta = 1.4 \times 10^{-9}$ GeV^{-1}(d). Lengths are given in units of the lattice spacing i.e. 10^{-10} GeV^{-1}.**

Spectrum of GWs after emission

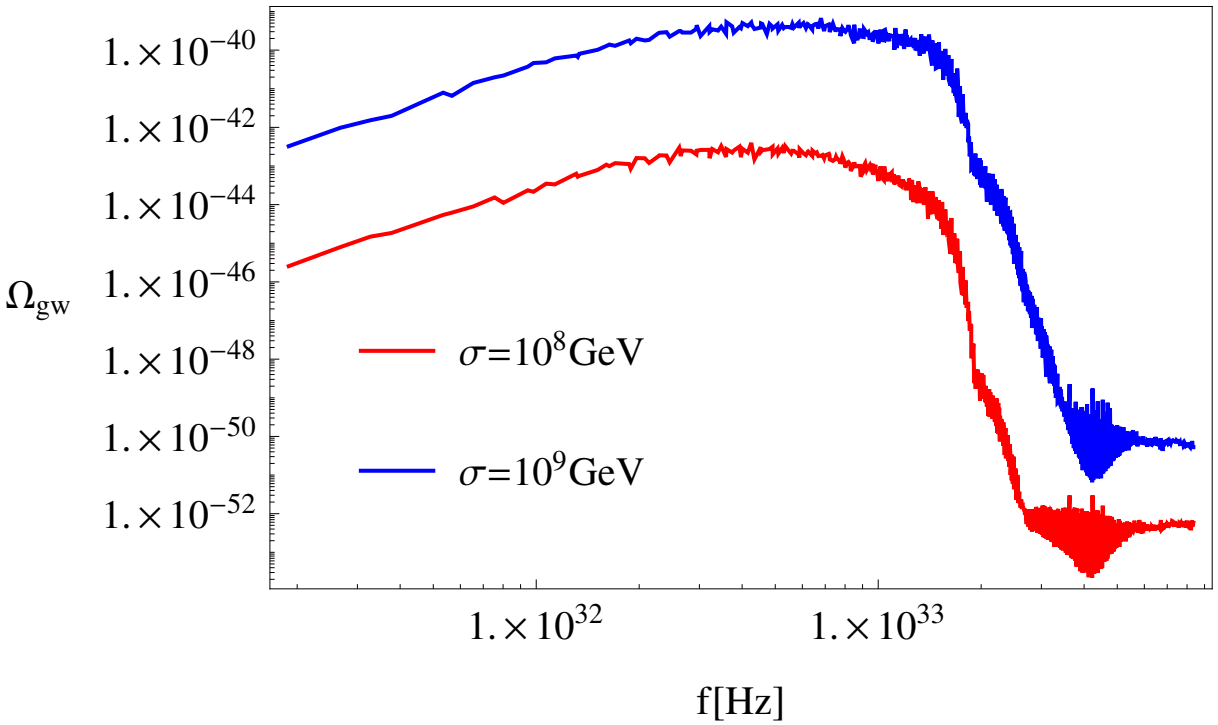

Figure: Spectrum of gravitational waves Ω_{gw} emitted from SM domain walls at the time of the decay.

Present spectrum of GWs

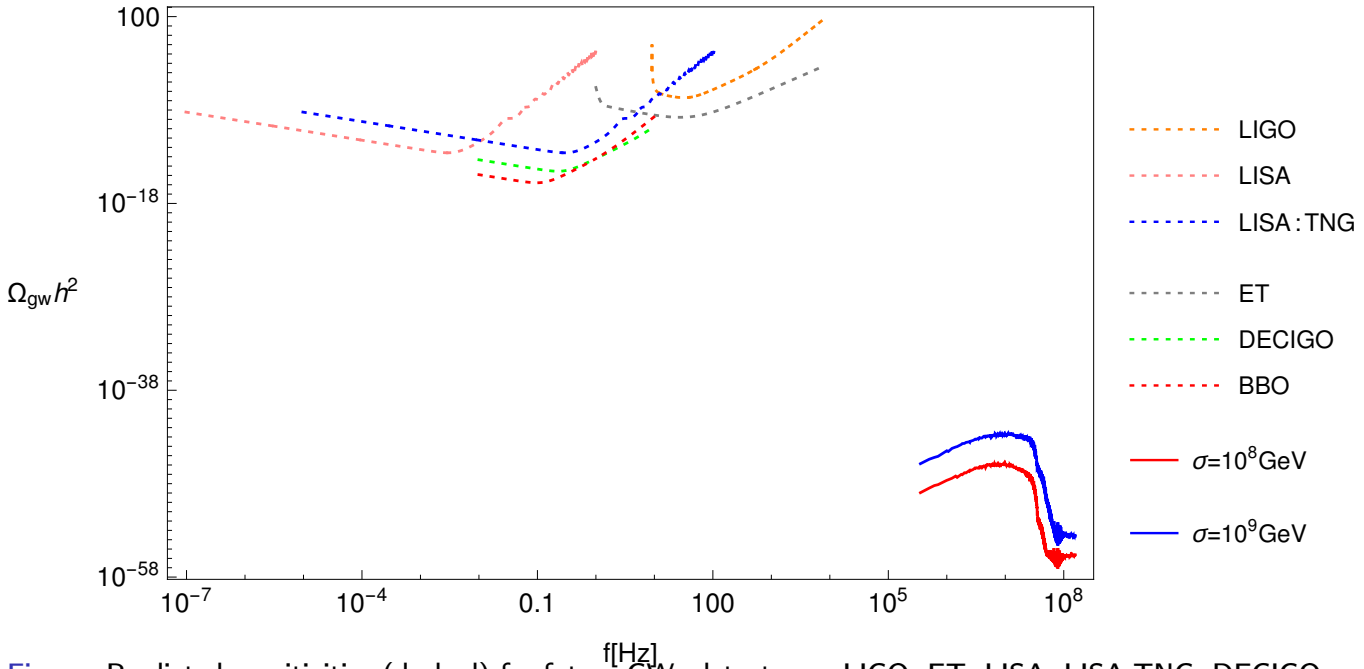

Figure: Predicted sensitivities (dashed) for future GWs detectors: aLIGO, ET, LISA, LISA:TNG, DECIGO and BBO compared with the spectrum of GWs (solid) calculated in lattice simulations for the initial values of $\sigma = 10^{8},\ 10^{9}\ \mathrm{GeV}$ and the standard cosmology.

New Physics and domain walls

New physics $\delta V_{SM}^{\Lambda}(h) = \frac{\lambda_6}{6!}\frac{h^6}{\Lambda_{NP}^2}$

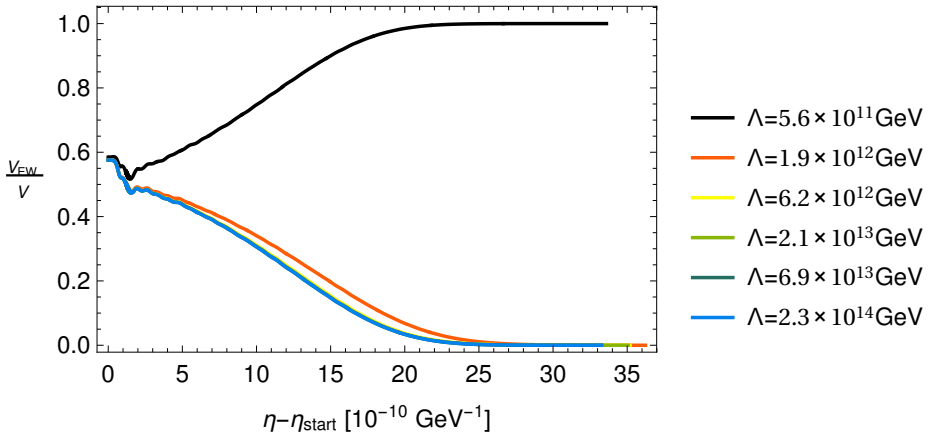

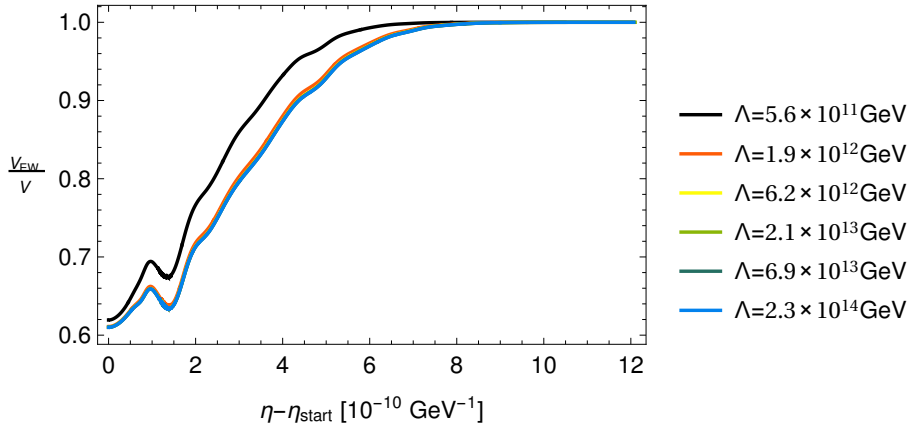

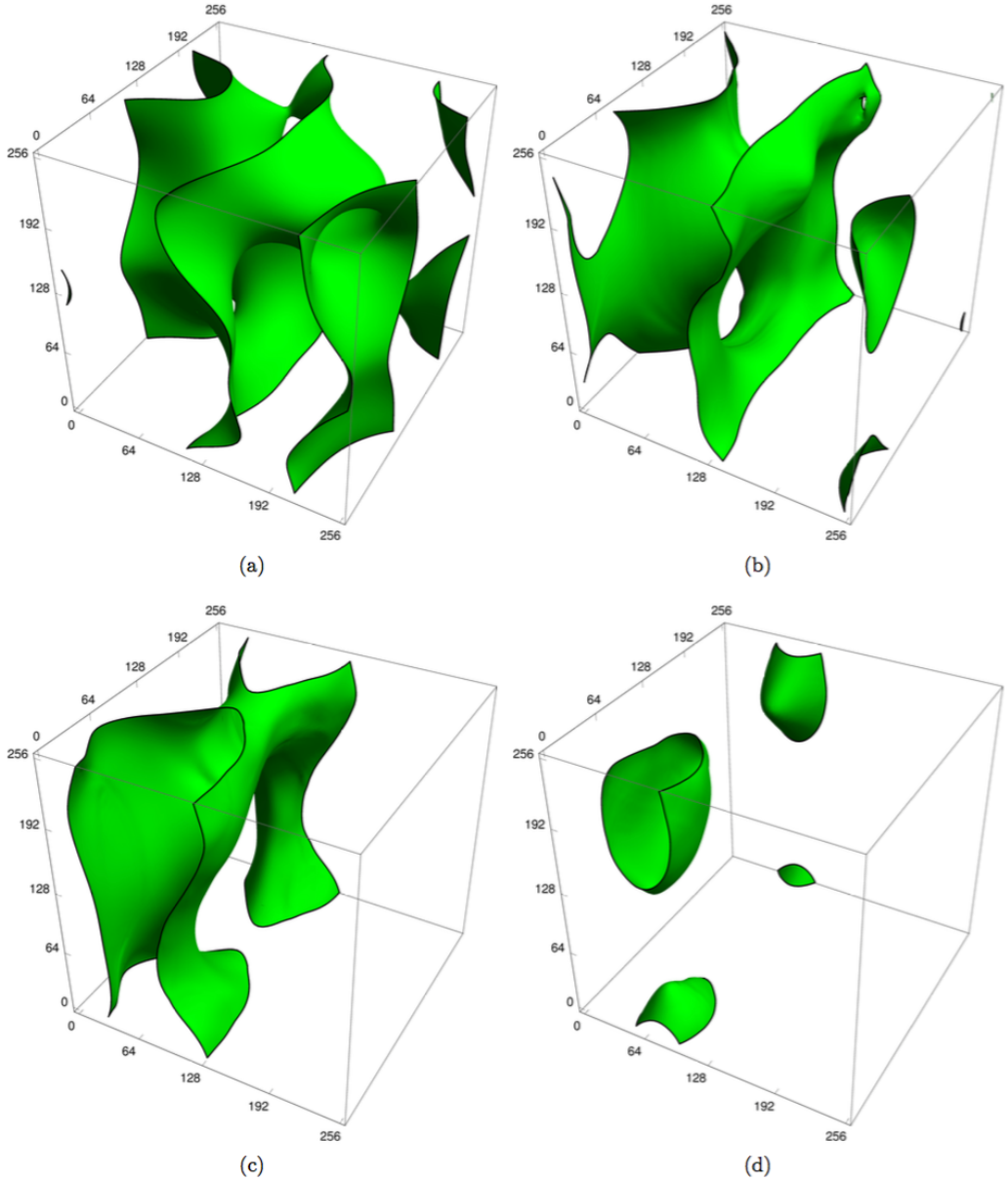

Figure 10: Visualization of the isosurface of the field strength ϕ corresponding to the value h_{max} at four different conformal times: $\eta = 1.41\times10^{-8}$ GeV^{-8} (a) and $\eta = 2.11\times10^{-8}$ GeV^{-1} (b), $\eta = 2.51 \times 10^{-8}$ GeV^{-1} (c), $\eta = 3.02 \times 10^{-8}$ GeV^{-1}(d). Lengths are given in units of the lattice spacing i.e. 10^{-10} GeV^{-1}.

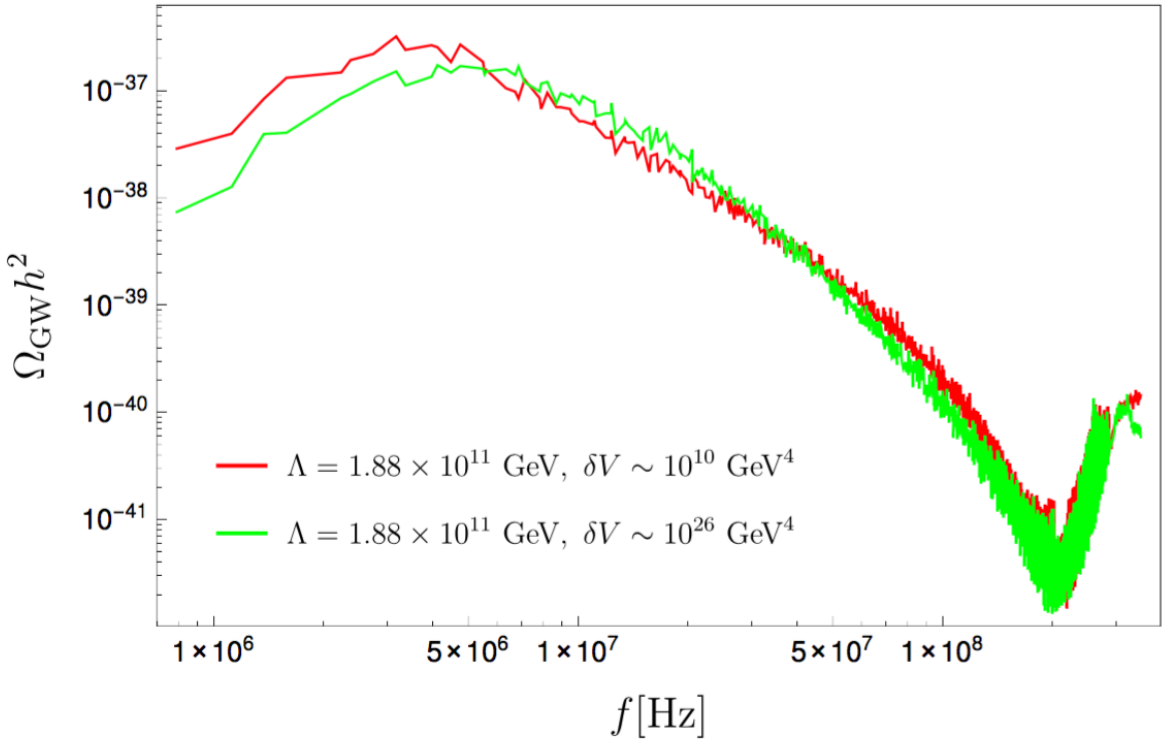

Figure 11: Present day spectrum of gravitational waves Ω_{gw} emitted from Higgs domain walls in the case of the Higgs potential with nearly degenerate minima with the difference in values of potential in minima of the order of $\delta V \sim 10^{10}$ GeV^4 (red) and $\delta V \sim 10^{26}$ GeV^4 (green).

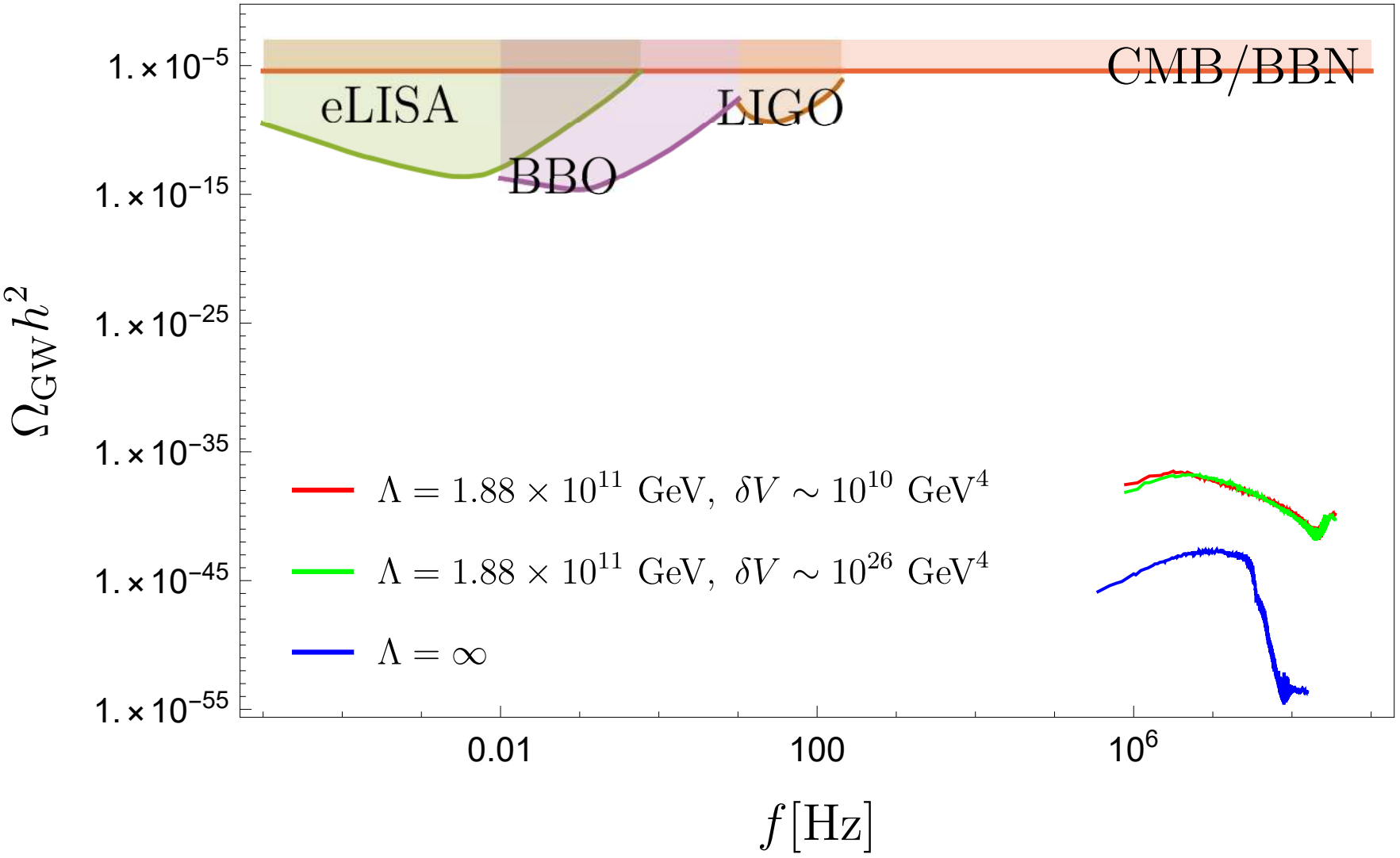
$1.\times10^{-5}$
$1.\times10^{-15}$
$1.\times10^{-25}$
$1.\times10^{-35}$
$1.\times10^{-45}$
$1.\times10^{-55}$
$\Omega_{\rm GW}h^2$
eLISA
BBO
LIGO
CMB/BBN
$\Lambda = 1.88\times10^{11}$ GeV, $\delta V \sim 10^{10}$ GeV^4
$\Lambda = 1.88\times10^{11}$ GeV, $\delta V \sim 10^{26}$ GeV^4
$\Lambda = \infty$
0.01
100
10^6
f [Hz]

Summary I

1. New Physics at scales higher than 10^{13} GeV does not influence Higgsa domain walls.
2. Networks of domain walls initialized with $\sigma < 3.25 \times 10^{10}$ GeV decay to the EWSB vacuum.
3. For lower values of the scale Λ lifetimes of Higgs domain walls are still short and smaller than 10^{-8} $\frac{\hbar}{\mathrm{GeV}}$ for generic inital configurations.
4. Thermal corrections to the effective potential stabilize the Higgs field by enlarging the basing of attraction of EWSB vacuum.
5. Higgs domain walls in the thermal background are highly unstable.
6. Gravitational waves produced from generic initial configurations are too weak to be detected in the planned detectors.

Generic asymmetric domain walls and gravitational waves

Models of interest

- Radiatively generated minima (eg SM at large field strength)

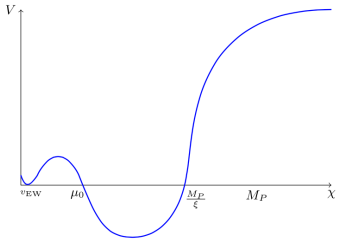

- Run-away potentials (moduli of stringy models), Quantum Scale Symmetric SM

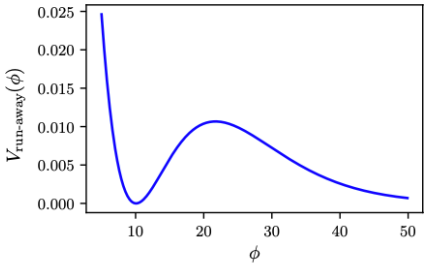

- Models of strong first-order phase transitions - colliding bubbles (thermal effects play a role)

Models of interest

- Monodromy axion models, relaxion

$$V_{\text{monodromy}}(\phi) = m^2\phi^2 + \Lambda^4\left[1 - \cos\left(\frac{\phi}{f}\right)\right]$$

$$V_{\text{relaxion}}(\phi) = g\phi + \Lambda^4\left[1 - \cos\left(\frac{\phi}{f}\right)\right]$$

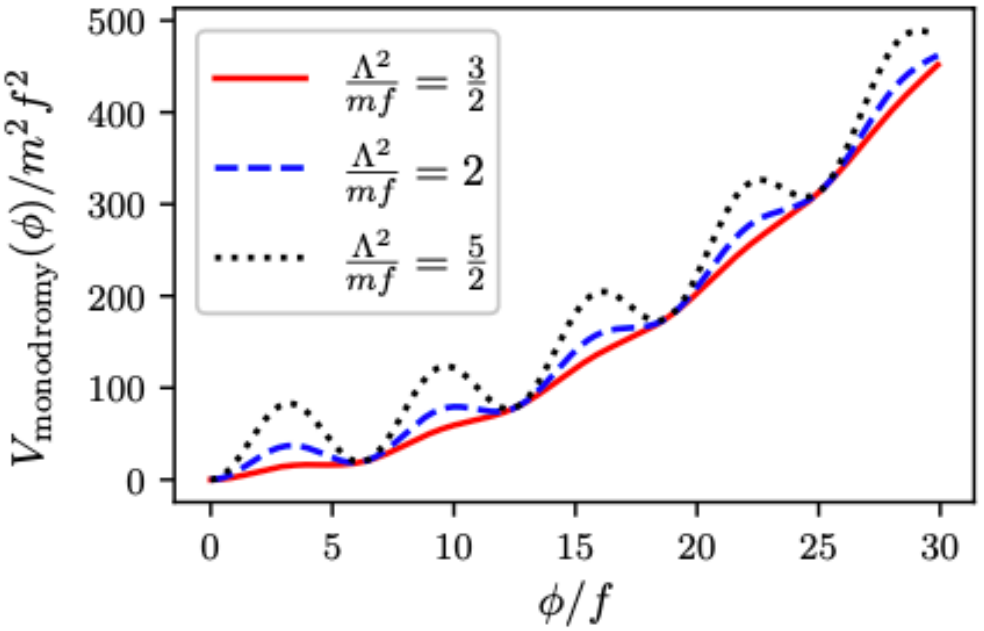

Generic potential

$$V_{AS}(\phi) = \frac{V_0}{60}\phi\left(15\phi^3\left(e^2\left(2d(a+b+c)+ab+ac+bc+d^2\right)+1\right)-60abc\left(d^2e^2+1\right)\right.$$
$$-20\phi^2\left(e^2\left(d^2(a+b+c)+2d(a(b+c)+bc)+abc\right)+a+b+c\right)-12e^2\phi^4(a+b+c+2d)$$
$$\left.+30\phi\left(de^2(ad(b+c)+2abc+bcd)+ab+ac+bc\right)+10e^2\phi^5\right). \quad (3.6)$$

$$\frac{\partial^3 V_{AS}}{\partial\phi^3}(\phi) = 2V_0\left(e^2(a-\phi)(\phi-b)(c+2d-3\phi)\right.$$
$$\left.+(-a-b+2\phi)\left(e^2(d-\phi)(2c+d-3\phi)+1\right)+(\phi-c)\left(e^2(d-\phi)^2+1\right)\right) \quad (3.$$

a, b - positions of minima, c - position of maximum

$$\delta V = V_{AS}(b) - V_{AS}(a),$$
$$d3V = \frac{\partial^3 V}{\partial\phi^3}(c),$$
$$5 = w,$$

Quanties of interest: energy density and peak frequency

$$\Omega_{GW}(\eta) := \frac{1}{\rho_c(\eta)} \frac{d\rho_{GW}}{d\log|k|}(\eta, k).$$

$$\Omega_{GW}(\eta_{dec})|_{peak} = \frac{\tilde{\epsilon}_{GW} \mathcal{A}^2 {\sigma_{wall}}^2}{24\pi {H_{dec}}^2 {M_{Pl}}^4},$$

$$\Omega_{GW}(\eta_0) = \left(\frac{a(\eta_{dec})}{a(\eta_0)}\right)^4 \left(\frac{H(\eta_{dec})}{H(\eta_0)}\right)^4 \Omega_{GW}(\eta_{dec})$$

Quanties of interest: energy density and peak frequency

$\tilde{\epsilon}_{GW}$ efficiency parameter between 0.7 and 1

σ_{walls}, η_{dec} - taken from simulations

$$\frac{A}{V} = \frac{a(t) S_{wall}}{H^{-3}} \propto \frac{a(t)}{t}.$$

$$\frac{A}{V} = \mathcal{A} \eta^{-1},$$

stable DW: $\mathcal{A}$ in the range 0.8 ± 0.1

Quanties of interest: energy density and peak frequency

more generally

$$\log\left(\frac{A}{V}\right) = -\nu \log \eta + \log \mathcal{A}$$

scaling regime: obtained ν ranges from 0.81 to 1.0

meta-stable DW: $\mathcal{A}$ in the range $0.08 - 0.34$

Scaling regime

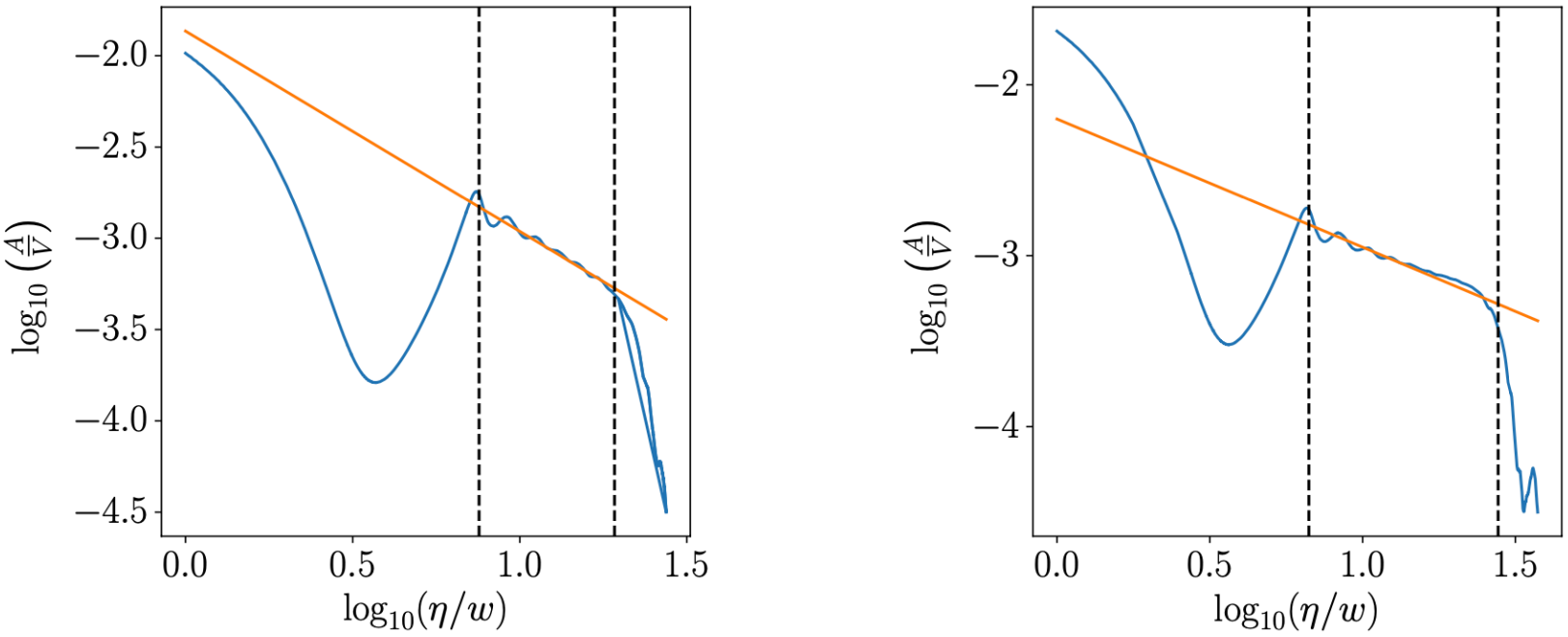

Figure 9: The evolution of conformal surface area of domain walls per unit volume $\frac{A}{V}$ in function of conformal time η (blue) and the fitted scaling behavior defined by eq. (5.8) (orange) for the best (left panel) and the worst (right panel) fits obtained by procedure described in the main text. Vertical dashed lines correspond to the estimated beginning and end of the scaling regime.

Quanties of interest: energy density and peak frequency

$$\Omega_{GW}(\eta_0)|_{peak} = 4.6 \times 10^{-81} \mathcal{A}^2 \left(\frac{\mathrm{GeV}}{H_{dec}}\right)^2 \left(\frac{\sigma_{wall}}{\mathrm{GeV}^3}\right)^2 h^{-2} \left(\frac{100}{g_*(\eta_{dec})}\right)^{\frac{1}{3}},$$

$$f_0|_{peak} = \frac{a(\eta_{dec})}{a(\eta_0)} H_{dec} = 1.63 \times 10^2 \left(\frac{H_{dec}}{\mathrm{GeV}}\right)^{\frac{1}{2}} \mathrm{Hz},$$

$$\Omega_{GW}(\eta_0)|_{peak} = 0.29 \times 10^{-77} \mathcal{A}^2 \left(\frac{\eta_{dec}}{w}\right)^4 \left(\frac{\sigma_{wall}}{w^{-3}}\right)^2 \left(\frac{\mathrm{GeV}^{-1}}{w}\right)^4,$$

$$f_0|_{peak} = 3.3 \times 10^1 \left(\frac{w}{\eta_{dec}}\right) \left(\frac{\mathrm{GeV}^{-1}}{w}\right)^{\frac{1}{2}} \mathrm{Hz},$$

Quanties of interest: energy density and peak frequency

We have estimated overall factors present in eqs. (6.7) and (6.7) basing on values of $\mathcal{A}$, η_{dec} obtained in simulations in which networks entered scaling regime and previously computed σ_{wall}. The maximal value of the prefactor in eq. (6.7) obtained in this way is equal to:

$$\Omega_{GW}^{max}(\eta_0)|_{peak} = 0.1 \times 10^{-66} \left(\frac{1 \frac{\hbar c}{\mathrm{GeV}}}{w} \right)^4, \qquad f_0^{max}|_{peak} = 0.7 \left(\frac{1 \frac{\hbar c}{\mathrm{GeV}}}{w} \right)^{\frac{1}{2}} \mathrm{Hz}, \tag{6.9}$$

where the frequency of the peak for this network is denoted as f_0^{max}. On the other hand, the minimal prefactor computed from data from simulations is equal to:

$$\Omega_{GW}^{min}(\eta_0)\big|_{peak} = 0.6 \times 10^{-68} \left(\frac{1 \frac{\hbar c}{\mathrm{GeV}}}{w} \right)^4, \qquad f_0^{min}\big|_{peak} = 1.3 \left(\frac{1 \frac{\hbar c}{\mathrm{GeV}}}{w} \right)^{\frac{1}{2}} \mathrm{Hz}. \tag{6.10}$$

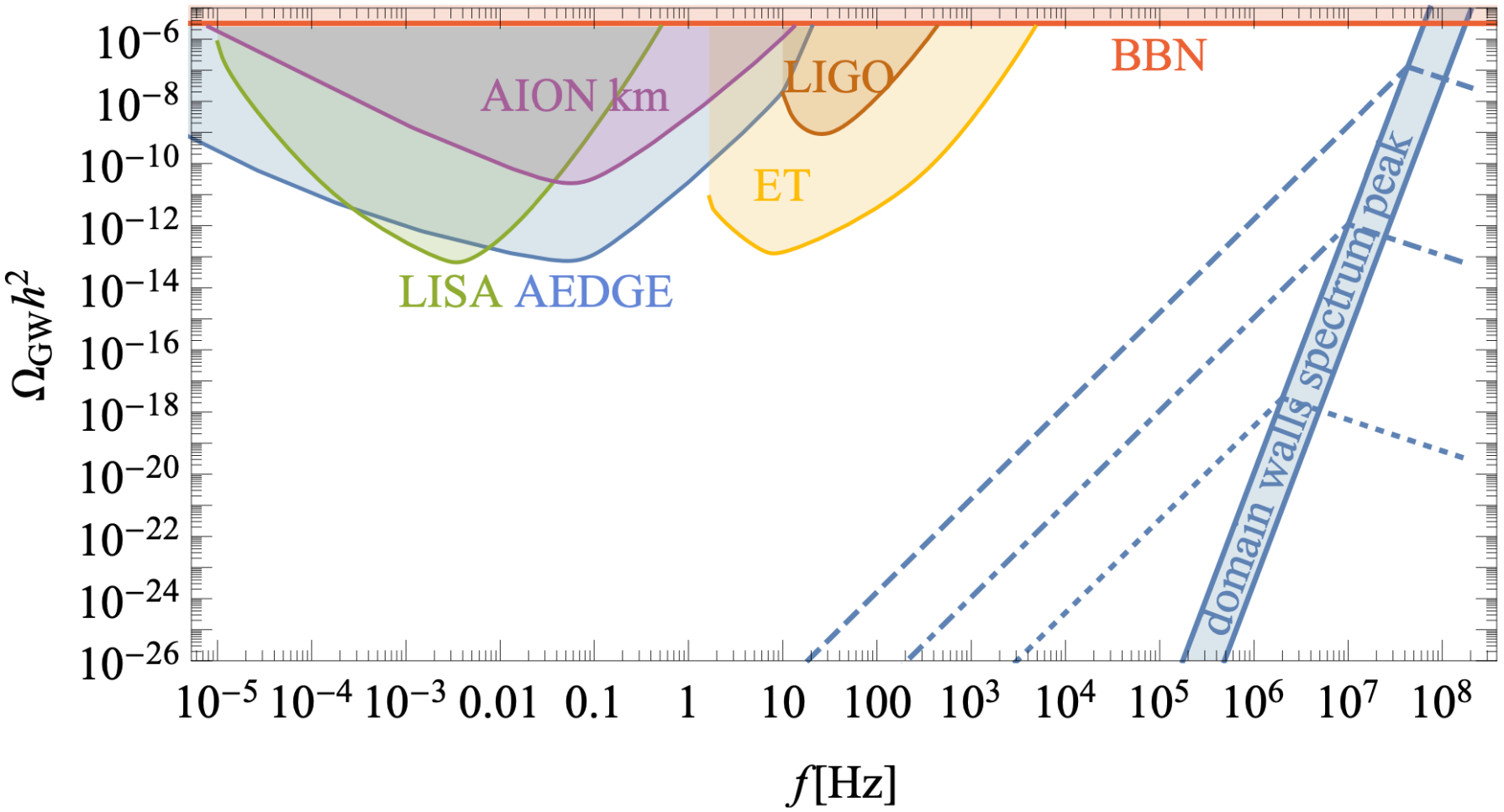

Figure 10: Hypothetical peak amplitudes of GWs emitted from cosmological domain walls as a function of the peak frequency f compared to predicted sensitivities of current and planned detectors LIGO [59–62], LISA [63, 64], AEDGE [65], AION-1km [66], ET [67, 68] as well as upper bound induced by the CMB/BBN [69, 70].

Summary II

- For a strong signal and a low frequency peak a period of stable evolution is needed
- Bias of the initial distribution easily destabilises the network
- Asymmetry of the potential destabilises the network for symmetric distributions
- Short living networks may give a strong signal if the energy scale is very large - but this produces a high frequency peak, beyond current sensitivity
- Decaying networks of domain walls produce a signal in the form of gravitational waves - too weak to be detected anytime soon - if a signal is detected then either fine-tuning or non-standard cosmology have occurred